

CHEMISTRY

A European Journal



Accepted Article

Title: Galactose-Grafted 2D Nanosheets from the Self-assembly of Amphiphilic Janus Dendrimers for the Capture and Agglutination of Escherichia coli

Authors: Nithiyandanan Krishnan, Devanathan Perumal, Siriki Atchimnaidu, Kaloos S. Harikrishnan, Murali Golla, Nilima Manoj Kumar, Jemshiya Kalathil, Jithu Krishna, Dileep K. Vijayan, and Reji Varghese

This manuscript has been accepted after peer review and appears as an Accepted Article online prior to editing, proofing, and formal publication of the final Version of Record (VoR). This work is currently citable by using the Digital Object Identifier (DOI) given below. The VoR will be published online in Early View as soon as possible and may be different to this Accepted Article as a result of editing. Readers should obtain the VoR from the journal website shown below when it is published to ensure accuracy of information. The authors are responsible for the content of this Accepted Article.

To be cited as: *Chem. Eur. J.* 10.1002/chem.201905228

Link to VoR: <http://dx.doi.org/10.1002/chem.201905228>

Supported by
ACES

WILEY-VCH

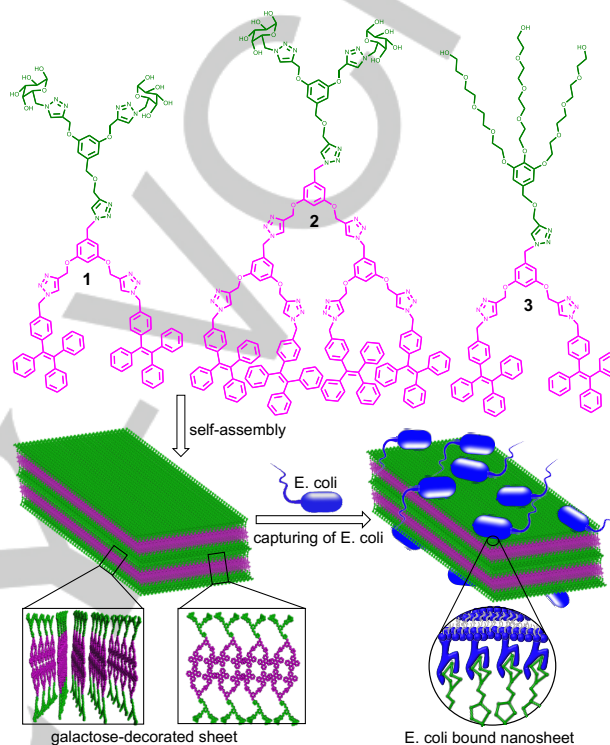
COMMUNICATION

Galactose-Grafted 2D Nanosheets from the Self-assembly of Amphiphilic Janus Dendrimers for the Capture and Agglutination of *Escherichia coli*

Nithyanandan Krishnan, Devanathan Perumal, Siriki Atchimnaidu, Kaloore S. Harikrishnan, Murali Golla, Nilima Manoj Kumar, Jemshiya Kalathil, Jithu Krishna, Dileep K. Vijayan, and Reji Varghese*

Abstract: High aspect ratio, sugar-decorated 2D nanosheets are the ideal candidate for the capture and agglutination of bacteria. Herein the design and synthesis of two carbohydrate-based Janus amphiphiles that spontaneously self-assemble into high aspect ratio 2D sheets are reported. The unique structural features of the sheet include the extremely high aspect ratio and dense display of galactose on the surface. These structural characteristics allow the sheet to act as a supramolecular 2D platform for the capturing and agglutination of *E. coli* through specific multivalent non-covalent interactions, which significantly reduces the mobility of the bacteria and leads to the inhibition of their proliferation. Our results suggest that the design strategy demonstrated here can be applied as a general approach for the crafting of biomolecule-decorated 2D nanosheet, which can perform as 2D platform for their interaction with specific targets.

Considerable attention has been paid by different research groups to understand and mimic the bacterial adhesion processes as this is the major pathway for many pathogenic bacteria to infect the host cell through multivalent host-guest interactions.^[1] Recent years have witnessed the emergence of several carbohydrates coated supramolecular nanostructures for bacterial capture. Zero-dimensional (0D) nanostructures such as dendrimers,^[2] nanoparticles^[3] and fullerenes^[4] have applied as scaffolds for the carbohydrate display and used for the interaction with bacteria. As expected, 1D nanostructures (e.g. carbon nanotubes^[5] and fibrous assemblies^[6]) were found to be more effective as scaffolds compared to 0D nanostructures. Lee *et al.* reported the efficient capturing of *Escherichia coli* (*E. coli*) by carbohydrate coated nanofiber and demonstrated the regulation of bacterial agglutination by tuning the fiber length.^[7] Undoubtedly, more efficient would be 2D nanosheets because of their extremely large surface area. Nevertheless, bacterial agglutination and inhibition of cell proliferation using 2D sheet as a scaffold received very little attention. Recently, Seeberger and Haag *et al.* demonstrated a multi-step strategy for the design of mannose functionalized graphene oxide as a 2D platform for the selective wrapping and agglutination of *E. coli*.^[8] Even more desirable would be a simple design that allows the creation of carbohydrate decorated 2D sheet in a single step self-assembly process. Zuckermann *et al.* reported an interesting case of self-assembly of carbohydrate functionalized peptoid into sheets having site-specific display of carbohydrates, which exhibited selective



Scheme 1. Chemical structures of amphiphiles 1–3 and schematic representation depicting the self-assembly of the amphiphile into sugar decorated, multi-layered 2D nanosheet. Capture and agglutination of *E. coli* onto the sheet through specific multivalent interaction are also shown. The benzene rings of TPE need not be fully planar in the aggregated state as shown.

binding to target proteins.^[9] However, the design of a supramolecular building block that spontaneously self-assembles into carbohydrate-coated, high aspect ratio, 2D nanosheet that can act as a multivalent ligand for the capturing, agglutination and inhibition of bacterial proliferation has not yet been achieved.

Amphiphilicity-driven self-assembly is a simple yet efficient bottom-up approach for the creation of soft nanostructures of defined morphology with tailored functionalities.^[10] Our group is interested in the self-assembly of amphiphiles, particularly DNA-based amphiphiles.^[11] We have shown that the incorporation of a large π -surface such as tetraphenylethylene (TPE)^[12] or hexabenzocoronene (HBC)^[13] as hydrophobic domains in the design of a DNA amphiphile drove the self-assembly into DNA-decorated 2D nanosheets. Motivated from these findings, we envisioned that the incorporation of a carbohydrate moiety as the hydrophilic segment to a large π -surface could drive the self-assembly of the amphiphile into carbohydrate-decorated 2D sheet, and hence they could perform as a potential multivalent ligand for the interaction with specific biomolecules.

[a] N. Krishnan, D. Perumal, S. Atchimnaidu, K. S. Harikrishnan, M. Golla, N. M. Kumar, J. Kalathil, J. Krishna, D. K. Vijayan and Dr. R. Varghese

School of Chemistry, Indian Institute of Science Education and Research (IISER) Thiruvananthapuram
Thiruvananthapuram-695551, India. E-mail: reji@iisertvm.ac.in

Supporting information for this article is given via a link at the end of the document. ((Please delete this text if not appropriate))

COMMUNICATION

Herein we report the design and synthesis of three (**1–3**) Janus amphiphiles that spontaneously self-assemble into high aspect ratio 2D sheets. The amphiphiles **1** and **2** consist of galactose dendron as the hydrophilic segment, which is conjugated to a hydrophobic tetraphenylethylene (TPE) dendron. Whereas the amphiphile **3** has tetraethylene glycol chains as the hydrophilic segment instead of galactose. TPE was selected in our study as the hydrophobe due to their unique optical properties and straightforward synthesis.^[14] Owing to the large π -surface of TPE dendron, the amphiphiles undergo strong π - π stacking in aqueous medium and spontaneously self-assemble into 2D sheet. The unique structural features of the sheets of **1** and **2** include the extremely high aspect ratio and dense display of galactose on their surface. These structural characteristics allow the sheet to act as a 2D platform for the efficient and selective capturing of *E. coli* and their agglutination through multivalent interaction between galactose and glycoproteins, protein expressed on the bacterial cell surface. This interaction significantly reduces the mobility of the bacteria and eventually leads to the inhibition of their proliferation. On the other hand, sheet derived from the self-assembly of **3** that has tetraethylene glycol on the surface shows no interaction with the bacteria, indicating that the specific interaction between the galactose and glycoproteins is solely responsible for the bacteria capture.

The only structural difference between the amphiphiles **1** and **2** is the difference in the hydrophobic dendron part. The amphiphile **1** has two TPE moieties, whereas **2** has four TPE moieties as the hydrophobic segments, and hence the hydrophobic surface area is larger for **2** compared to **1**. Self-assembly of the amphiphile was achieved by the gradual addition of water into a DMSO solution of the amphiphile (water:DMSO = 98:2). All experiments were done at a concentration of 10 μ M. Absorption spectra of **1** and **2** in DMSO showed a broad band with λ_{max} at 307 nm, which corresponds to the π - π^* transition of TPE (Figure S1). Interestingly, red-shifts of 13 nm and 10 nm were observed with the addition of water into the DMSO solution of **1** and **2**, respectively. These observations suggest that **1** and **2** exist as monomeric species in DMSO and undergo aggregation with the addition of water mainly through π - π stacking interactions. Moreover, **1** and **2** are weakly emissive in DMSO with fluorescence quantum yields of 0.05 and 0.04, respectively. Interestingly, a dramatic increase in emission intensity with a concomitant red-shift of 100 nm was observed for the aggregated species of **1** and **2** (376 \rightarrow 476 nm) (Figure 1a and Figure S2). The fluorescence quantum yields for the aggregated species of **1** and **2** are 0.4 and 0.5, respectively. These results imply that the weak emission for the monomeric species of **1** and **2** is due to the intramolecular C(sp²)-C(sp²) bond rotational relaxation of TPE, whereas restriction of rotational relaxation in the aggregated state enhances the emission.^[14]

Atomic force microscopic (AFM) analyses revealed that the aggregates formed in solution are high aspect ratio 2D sheets (Figure 1b). Section analyses showed that the lateral width of the sheets of **1** and **2** are in the range of several hundred nanometers to micrometers (Figure 1b inset). Heights of the sheets are in the range of 12–150 nm and 16–270 nm for **1** and **2**, respectively, which is significantly larger than the calculated bilayer thicknesses of **1** (~3.2 nm) and **2** (~4.6 nm). Large thickness of the sheet points to a possible layer-by-layer assembly of the

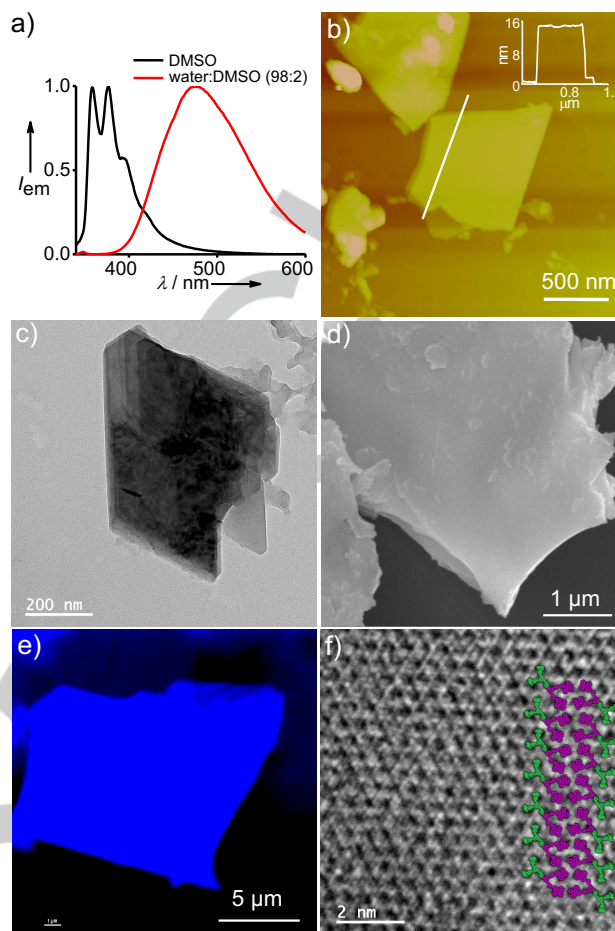


Figure 1. a) Normalized fluorescence spectra of **1** in DMSO (black) and water:DMSO (red). b) AFM, c) TEM, d) SEM, e) confocal microscopic and f) HR-TEM images of sheet of **1**. The inset of AFM image shows the corresponding section analysis of the sheet. A possible bilayer organization of the amphiphile is shown on the HR-TEM image.

sheets through H-bonding interactions of the galactose moieties protruded on the sheet surface. Even at a low concentration of 1 μ M, multilayered sheets were dominated. However, we could observe population of sheets with thickness of ~3 and ~4 nm for **1** and **2**, respectively (Figure S5). Since the observed heights are approximately matching with the corresponding bilayer distances of **1** and **2**, these results support a lamellar assembly for the amphiphiles. Fourier-transform infrared spectroscopy analyses of the sheets showed significant red-shifts and broadening of O-H stretching vibration of galactose when compared to the corresponding monomeric species. Red-shifts of 272 cm^{-1} (3693 \rightarrow 3421 cm^{-1}) and 281 cm^{-1} (3695 \rightarrow 3414 cm^{-1}) were respectively observed for **1** and **2** sheets (Figure S6 and S7), which can be attributed to the H-bonding interaction between galactose. This confirms the layer-by-layer assembly of the sheets. Scanning electron (SEM) and transmission electron microscopic (TEM) analyses also confirmed the formation of high aspect ratio sheets for **1** (Figure 1c and d) and **2** (Figure S9 and S11). Interestingly, confocal microscopic analyses revealed that the lateral width of the sheets are extremely large and are in the range of 10–100 μ m (Figure 1e).

COMMUNICATION

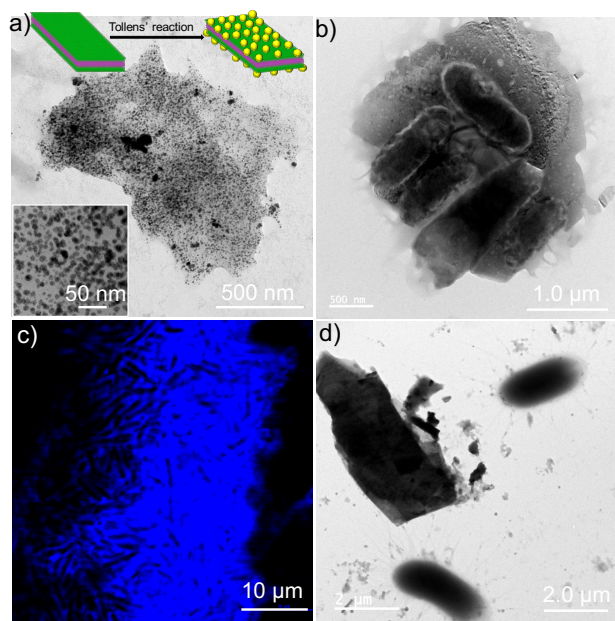


Figure 2. a) TEM image of the in-situ formed AgNPs on the sheet of **1** using the Tollens' reaction and a schematic for this reaction is also shown. b) TEM and c) confocal microscopic images of *E. coli* captured onto the sheet of **1**. d) TEM image of the interaction of *E. coli* with sheet of **3**.

Remarkably, high resolution TEM image of sheet of **1** clearly resolved the lamellar and layer-by-layer assembly of the amphiphiles (Figure 1f) and the observed bilayer distance of ~3 nm is approximately matching with the calculated distance (~3.2 nm). However, we were unable to molecularly resolve the structure of sheet of **2**. Furthermore, broad diffraction peaks at $2\theta = 17\text{--}24^\circ$ ($d = 5.2\text{--}3.7 \text{ \AA}$) and $16\text{--}23^\circ$ ($d = 5.5\text{--}3.8 \text{ \AA}$) were observed for the sheets of **1** (Figure S14a) and **2** (Figure S14b) in the powder X-ray diffraction analyses, respectively. These peaks could be assigned to different $\pi\text{--}\pi$ stacking distance of TPE segments in the multilayered sheet. Based on all these analyses, a plausible model for the self-assembly of the amphiphiles is depicted in Scheme 1.

The surface display of galactose on the sheet was unambiguously confirmed using the well-known Tollens' reaction, which involves the reduction of Ag⁺ to silver nanoparticles (AgNPs) using galactose as the reducing agent. To this end, Tollens' reagent ([Ag(NH₃)₂]⁺) (100 μM) was added to the galactose decorated sheets of **1** or **2** (10 μM), vortexed for 2 h in dark and filtered. The reaction was monitored using electronic spectroscopy and it was observed that within an hour, a new band started appearing at 330–670 nm, corresponding to the surface plasmonic absorption band of AgNPs (Figure S15). A gradual increase in intensity of this band was observed with time and got saturated at 2 h. These results imply that the galactose moieties protruded on the sheet surface act as a reducing agent for the reduction of Ag⁺ to AgNPs.^[15] In support of this, a significant quenching of fluorescence of TPE was observed due to the electronic interaction between AgNPs on the sheet and TPE. This is possible as the distance separating the NPs and TPE is only ~2 nm (for **1**). Nanoparticle formation was further confirmed by TEM

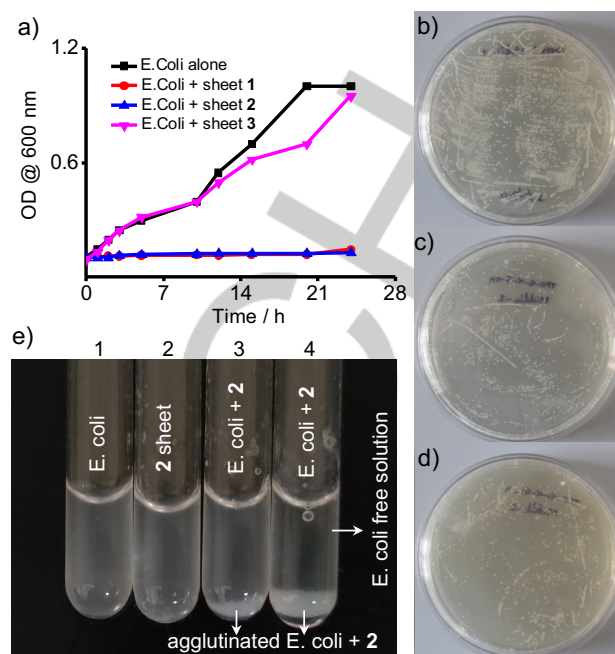


Figure 3. a) Changes of optical density at 600 nm for *E. coli* alone and *E. coli* treated with **1–3** sheets. Images of *E. coli* bacterial colonies: b) *E. coli* alone (control), c) *E. coli* treated with sheet of **1** and d) *E. coli* treated with sheet of **2**. e) Images of *E. coli* contaminated water treated with **2** sheets. The vials 1–4 represent *E. coli*, sheet of **2**, *E. coli* treated with sheets of **2** (0.2 mM) and *E. coli* treated with sheets of **2** (0.3 mM), respectively.

analyses, which showed the formation of NPs (~5 nm) that are randomly deposited on the surface of the sheet (Figure 2a).

Motivated from the large surface area of the sheet and dense display of galactose on the surface, we then explored the potential of the sheet as a multivalent 2D scaffold for the capturing and agglutination of bacteria. Cytotoxicity of the sheets was studied using 3-(4,5-dimethylthiazol-2-yl)-2,5-diphenyltetrazolium bromide (MTT) assay. For this purpose, sheets ($c = 10 \mu\text{M}$) were treated with A549 (cancer) and HEK 293 (normal) cell lines for 24 h and the subsequent MTT assay revealed that no toxicity was associated with the sheets (Figure S18). After confirming the biocompatibility of the sheets, their potential as a multivalent ligand for the capturing of gram-negative *E. coli* (DH5 α strain) was studied. Nanosheets of **1** was treated with *E. coli* cells for 24 h. TEM analyses revealed the clustering of bacteria on the sheet (Figure 2b). It is also worth noting that the sheet morphology was found to be intact even after binding of the bacteria, proving the structural robustness of the sheet. Interestingly, confocal laser scanning microscopic (CLSM) analyses clearly showed the agglutination of bacteria, where bacteria appear as dark features on blue emissive sheet (Figure 2c). Agglutination was further confirmed with SEM (Figure S21) and AFM (Figure S22) analyses. Interestingly, nanosheet derived from the self-assembly of amphiphile **3** (Figure S25), which has tetraethylene glycol as the hydrophilic segment instead of galactose, showed no interaction with the bacteria as evident from TEM analyses (Figure 2d). This shows that specific multivalent interaction of *E. coli* with galactose is responsible for the capturing of bacteria onto the sheet.

COMMUNICATION

The ability of the sheet to capture and inhibit the growth of the bacteria was studied by monitoring the changes of optical density at 600 nm using a microplate reader. For this, *E. coli* was cultured alone (control) and along with 1/2/3 nanosheets for 24 h. As expected, normal bacterial growth was observed for *E. coli* alone and *E. coli* treated with sheets of **3**. On the other hand, a significant reduction in the growth of the bacteria was observed for *E. coli* treated nanosheets of **1** and **2**. Agglutination Index (AI) calculated from 20 random fields of microscopic images (TEM and CLSM) showed high AI values of 60 and 62 for the sheets of **1** and **2**, respectively, which are higher than those reported for similar supramolecular systems.^[6c] Inhibition of bacterial growth was further supported by plate-counting technique. For this, *E. coli* was cultured alone (control) and along with 1/2 nanosheets for 24 h, spread over agar plate and the colony-forming ability was monitored over a period of time. Colony counting showed a normal growth for *E. coli* (Figure 3b), whereas significant inhibition of bacterial growth was observed for *E. coli* treated with sheets of **1** and **2** (Figure 3c and 3d). These results fully support our hypothesis that the galactose decorated sheet allow the efficient capturing of bacteria through specific multivalent interaction between galactose protruded on the sheet and galactose binding protein in the bacterial pili of DH5 α strain. This leads to the agglutination of bacteria that prevent the motility and further growth of the bacteria. We have also demonstrated the potential of the sheet to capture and remove bacteria from water that was artificially contaminated with *E. coli*. This was shown by treating the bacteria contaminated water with sheets of **2** at two different concentrations (0.2 and 0.3 mM) in PBS buffer (pH 7.5) and kept undisturbed for 4 h. Agglutination followed by sedimentation of the bacteria was clearly observed for both the concentrations of **2** (Figure 3e, vials 3 and 4), and as expected the sheets of high concentration exhibited efficient bacterial capture (Figure 3e, vial 4). Furthermore, turbid bacteria solution became very clear after bacterial capture, whereas no sedimentation of bacteria was observed for *E. coli* alone (Figure 3e, vial 1).

In summary, we have reported the design and synthesis of a new class of carbohydrate-based Janus amphiphiles that spontaneously self-assemble into high aspect ratio, galactose-decorated nanosheets. We have also shown the potential of 2D sheet to act as a multivalent ligand for the capturing and agglutination of bacteria through specific host-guest interaction. To our knowledge, this is the first report demonstrating the crafting of sugar-grafted, high aspect ratio, 2D sheet from the self-assembly of sugar-based Janus amphiphile that efficiently capture, agglutinate and inhibit the growth of bacteria. This study indisputably suggests that the carbohydrate-decorated 2D sheets having large surface area are indeed a promising class of nanostructures for the interaction with bacteria, and our results are expected to open up further research interest towards the development of antibacterial nanomaterials.

Acknowledgements

Financial supports from DBT and KSCSTE are gratefully acknowledged. We thank UGC and CSIR for research fellowships. D. K. V. thanks IISER for a post-doc fellowship.

Keywords: self-assembly • amphiphiles • 2D materials • bacterial capture • fluorescence

- [1] a) A. Gupta, S. Mumtaz, C.-H. Li, I. Hussain, V. M. Rotello, *Chem. Soc. Rev.* **2019**, *48*, 415–427; b) S. Bhatia, L. C. Camacho, R. Haag, *J. Am. Chem. Soc.* **2016**, *138*, 8654–8666.
- [2] a) K. H. Schlick, C. K. Lange, G. D. Gillispie, M. J. Cloninger, *J. Am. Chem. Soc.* **2009**, *131*, 16608–16609; b) S. Zhang, R.-O. Moussoadia, H.-J. Sun, P. Leowanawat, A. Muncan, C. D. Nusbaum, K. M. Chelling, P. A. Heiney, M. L. Klein, S. André, R. Roy, H.-J. Gabius, V. Percec, *Angew. Chem.* **2014**, *126*, 11079–11083; *Angew. Chem. Int. Ed.* **2014**, *53*, 10899–10903.
- [3] a) K. El-Boubbou, C. Gruden, X. Huang, *J. Am. Chem. Soc.* **2007**, *129*, 13392–13393; b) R. L. Phillips, O. R. Miranda, C.-C. You, V. M. Rotello, U. H. F. Bunz, *Angew. Chem.* **2008**, *120*, 2628–2632; *Angew. Chem. Int. Ed.* **2008**, *47*, 2590–2594; c) K. Petkau, A. Kaeser, I. Fischer, L. Brunsveld, A. P. H. J. Schenning, *J. Am. Chem. Soc.* **2011**, *133*, 17063–17071.
- [4] a) P. Compain, C. Decroocq, J. Iehl, M. Holler, D. Hazelard, T. Mena Barragán, C. O. Mellet, J.-F. Nierengarten, *Angew. Chem.* **2010**, *122*, 5889–5892; *Angew. Chem. Int. Ed.* **2010**, *49*, 5753–5756; b) A. Muñoz, D. Sigwalt, B. M. Illescas, J. Luczkowiak, L. Rodríguez-Pérez, I. Nierengarten, M. Holler, J.-S. Remy, K. Buffet, S. P. Vincent, J. Rojo, R. Delgado, J.-F. Nierengarten, N. Martín, *Nat. Chem.* **2016**, *8*, 50–57.
- [5] a) H. Wang, L. Gu, Y. Lin, F. Lu, M. J. Mezziani, P. G. Luo, W. Wang, L. Cao, Y.-P. Sun, *J. Am. Chem. Soc.* **2006**, *128*, 13364–13365; b) G. Yu, J. Li, W. Yu, C. Han, Z. Mao, C. Gao, F. Huang, *Adv. Mater.* **2013**, *25*, 6373–6379.
- [6] a) J.-H. Ryu, E. Lee, Y.-b. Lim, M. Lee, *J. Am. Chem. Soc.* **2007**, *129*, 4808–4814; b) M. K. Müller, L. Brunsveld, *Angew. Chem.* **2009**, *121*, 2965–2968; *Angew. Chem. Int. Ed.* **2009**, *48*, 2921–2924; c) G. Yu, Y. Ma, C. Han, Y. Yao, G. Tang, Z. Mao, C. Gao, F. Huang, *J. Am. Chem. Soc.* **2013**, *135*, 10310–10313.
- [7] D.-W. Lee, T. Kim, I.-S. Park, Z. Huang, M. Lee, *J. Am. Chem. Soc.* **2012**, *134*, 14722–14725.
- [8] Z. Qi, P. Bharate, C.-H. Lai, B. Ziem, C. Böttcher, A. Schulz, F. Beckert, B. Hatting, R. Mülhaupt, P. H. Seeberger, R. Haag, *Nano Lett.* **2015**, *15*, 6051–6057.
- [9] A. Battigelli, J. H. Kim, D. C. Dehigaspitiya, C. Proulx, E. J. Robertson, D. J. Murray, B. Rad, K. Kirshenbaum, R. N. Zuckermann, *ACS Nano* **2018**, *12*, 2455–2465.
- [10] a) J. P. Hill, W. Jin, A. Kosaka, T. Fukushima, H. Ichihara, T. Shimomura, K. Ito, T. Hashizume, N. Ishii, T. Aida, *Science* **2004**, *304*, 1481–1483; b) J. F. Hulvat, M. Sofos, K. Tajima, S. I. Stupp, *J. Am. Chem. Soc.* **2005**, *127*, 366–372; c) F. J. M. Hoeben, I. O. Shklyarevskiy, M. J. Pouderoijen, H. Engelkamp, A. P. H. J. Schenning, P. C. M. Christianen, J. C. Maan, E. W. Meijer, *Angew. Chem.* **2006**, *118*, 1254–1258; *Angew. Chem. Int. Ed.* **2006**, *45*, 1232–1236; d) E. Lee, J.-K. Kim, M. Lee, *Angew. Chem.* **2009**, *121*, 3711–3714; *Angew. Chem. Int. Ed.* **2009**, *48*, 3657–3660; e) M. A. Azagarsamy, P. Sockalingam, S. Thayumanavan, *J. Am. Chem. Soc.* **2009**, *131*, 14184–14185; f) F. García, L. Sánchez, *Chem. Eur. J.* **2010**, *16*, 3138–3146; g) B. Narayan, S. P. Senanayak, A. Jain, K. S. Narayan, S. J. George, *Adv. Funct. Mater.* **2013**, *23*, 3053–3060; h) C. Rest, M. J. Mayoral, K. Fucke, J. Schellheimer, V. Stepanenko, G. Fernández, *Angew. Chem.* **2014**, *126*, 716–721; *Angew. Chem. Int. Ed.* **2014**, *53*, 700–705; i) X. Zhang, D. Görl, V. Stepanenko, F. Würthner, *Angew. Chem.* **2014**, *126*, 1294–1298; *Angew. Chem. Int. Ed.* **2014**, *53*, 1270–1274; j) S. Yagai, S. Okamura, Y. Nakano, M. Yamauchi, K. Kishikawa, T. Karatsu, A. Kitamura, A. Ueno, D. Kuzuhara, H. Yamada, T. Seki, H. Ito, *Nat. Commun.* **2014**, *5*, 4013; k) V. S. Talens, P. Englebienne, T. T. Trinh, W. E. M. Noteborn, I. K. Voets, R. E. Kielytyka, *Angew. Chem.* **2015**, *127*, 10648–10652; *Angew. Chem. Int. Ed.* **2015**, *54*, 10502–10506; l) S. Ghosh, D. S. Philips, A. Saeki, A. Ajayaghosh, *Adv. Mater.* **2017**, *29*, 1605408–1605408.

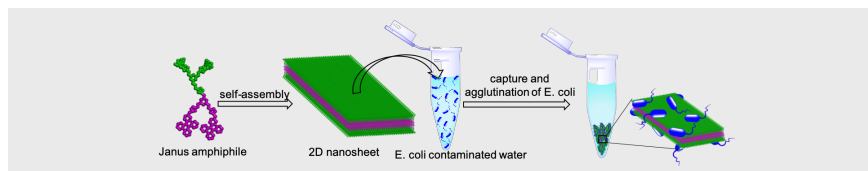
COMMUNICATION

- [11] a) S. K. Albert, H. V. P. Thelu, M. Golla, N. Krishnan, S. Chaudhary, R. Varghese, *Angew. Chem.* **2014**, *126*, 8492–8497; *Angew. Chem. Int. Ed.* **2014**, *53*, 8352–8357; b) M. Golla, S. K. Albert, S. Atchimnaidu, D. Perumal, N. Krishnan, R. Varghese, *Angew. Chem.* **2019**, *131*, 3905–3909; *Angew. Chem. Int. Ed.* **2019**, *58*, 3865–3869.
- [12] N. Krishnan, M. Golla, H. V. P. Thelu, S. K. Albert, S. Atchimnaidu, D. Perumal, R. Varghese, *Nanoscale* **2018**, *10*, 17174–17181.
- [13] S. K. Albert, I. Sivakumar, M. Golla, H. V. P. Thelu, N. Krishnan, J. Libin K. L., Ashish, R. Varghese, *J. Am. Chem. Soc.* **2017**, *139*, 17799–17802.
- [14] Y. Hong, J. W. Y. Lam, B. Z. Tang, *Chem. Soc. Rev.* **2011**, *40*, 5361–5388.
- [15] R. Dondi, W. Su, G. A. Griffith, G. Clark, G. A. Burley, *Small* **2012**, *8*, 770–776.

COMMUNICATION

Entry for the Table of Contents (Please choose one layout)

COMMUNICATION



Amphiphilicity-driven self-assembly of galactose-based Janus amphiphiles into galactose-decorated 2D nanosheet, which can efficiently capture and agglutinate *E. coli* through specific multivalent interactions between galactose and galactose binding protein in the bacterial pili of *E. coli* DH5 α strain is reported.

*N. Krishnan, D. Perumal, S. Atchimnaidu, K. S. Harikrishnan, M. Golla, N. M. Kumar, J. Kalathil, J. Krishna, D. K. Vijayan, R. Varghese**
Page No. – Page No.

Galactose-Grafted 2D Nanosheets from the Self-assembly of Amphiphilic Janus Dendrimers for the Capture and Agglutination of Escherichia coli